Kinetics and Modeling of Diethylene Glycol Bisallyl Carbonate Bulk Polymerization

Iztok Hace, Janvit Golob, Matjaž Krajnc

Faculty of Chemistry and Chemical Technology, University of Ljubljana, Aškerčeva 5, P.O. Box 537, SI-1001 Ljubljana, Slovenia

Received 15 June 2004; accepted 16 September 2004
DOI 10.1002/app.21418
Published online in Wiley InterScience (www.interscience.wiley.com).

ABSTRACT: The free-radical polymerization kinetics of diethylene glycol bisallyl carbonate in bulk were investigated with Fourier transform infrared and Fourier transform Raman techniques in a wide temperature range of 50–140°C with four different peroxide initiators. In addition, the ratios of the degradative kinetic rate constant to the propagation rate constant under different reaction conditions were obtained from molecular weight measurements under various reaction conditions. The ratio of the chemically controlled termination and propagation rate constants of the polymerization system were obtained with the initial rates of polymerization and the number-average molecular weight data, which were between 8.22×10^{-5} and 1.47×10^{-3} L mol^{-1} s^{-1}. The initiator efficiencies were evaluated with special experiments at low initiator concentrations with the theory of dead-end polymerization. The computed conversions from the developed kinetic model were in good agreement with the conversion and molecular weight measured data. The values of the diffusion-controlled propagation and termination rate constants, with clear and physical meaning, were the only two parameters obtained from the developed kinetic model fitting the measured conversion points. © 2005 Wiley Periodicals, Inc. J Appl Polym Sci 96: 345–357, 2005

Key words: diffusion; modeling; monomers

INTRODUCTION

The polymerization of diethylene glycol bisallyl carbonate (DADC), which is also known as CR-39, initiated by various peroxide initiators such as benzoyl peroxide (BPO) and isopropyl peroxydicarbonate, has been well investigated in the past[1–4] with various analytical techniques. Industrial interest in CR-39 is particularly strong in the optical industry, especially for the production of optical lenses because of its good optical properties.[2] Schnarr and Russell[1] investigated the polymerization of DADC at low conversions by measuring the molecular weights and polymer structure with Fourier transform infrared (FTIR) and NMR. O'Donnell and O'Sullivan[3] measured DADC polymerization with 3 wt % BPO as the initiator with Fourier transform Raman (FT-Raman) spectroscopy up to high conversions, and they observed first-order kinetics. Hill et al.[4] studied CR-39 polymerization initiated by various peroxide initiators with electron spin resonance (ESR) spectroscopy and compared the results with those for other multiallyl monomers.[4] In addition, Hill et al.[2,4] proposed a kinetic scheme for bulk CR-39 polymerization and evaluated some of the main kinetic rate constants by measuring the radical and C═C double-bond concentrations. Matsumoto et al.,[5] in their continuous study of multiallyl monomers, proposed a detailed kinetic scheme for DADC polymerization, which also included the appearance of cyclization reactions. Based on these studies, various kinetic models for DADC bulk polymerization have already been proposed.[1–5] However, a kinetic model with parameters with clear and physical meaning cannot be found in the available literature.

The polymerization of DADC consists of three main kinetic stages: the initiation of the monomer, propagation, and termination. In addition, the degradative chain transfer, reinitiation, and stabilization of active radical reactions occur, and this cannot be neglected.[5,6] Possible side cyclization reactions are another factor making DADC polymerization even more interesting.[1,5] Schnarr and Russell[1] reported that cyclization is only of minor importance in DADC polymerization because of the formation of 16 cycled rings during the reaction, and so the cyclization can be neglected in the reaction scheme.[1] In addition, Perera[7] confirmed with NMR measurements that the extent of cyclization is only 10% in the polymerization of CR-39. Matsumoto[6] observed the appearance of high diffusion limitations during bulk DADC polymerization; this was similar to what was reported for other multiallyl monomers.

Correspondence to: M. Krajnc (matjaz.krajnc@uni-lj.si).
Contract grant sponsor: Slovenian Ministry of Education, Science, and Sport; contract grant sponsor: L2-3539.

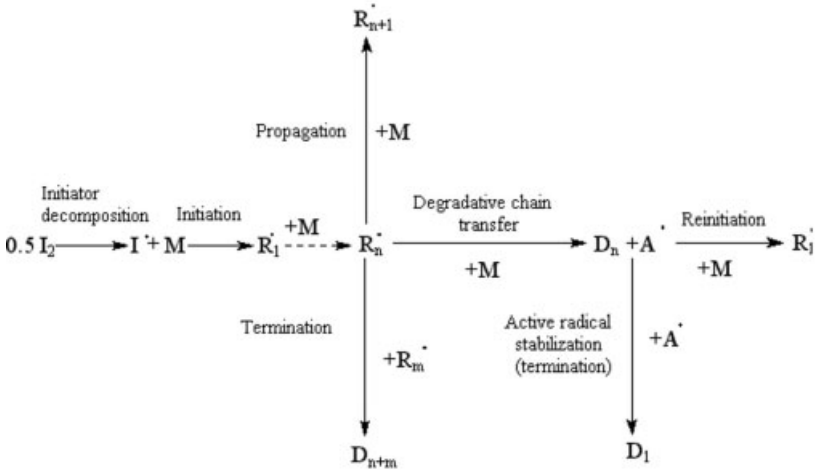

Figure 1 Reaction pathway.

In this article, the results of our experimental investigation and model simulation of bulk DADC polymerization over a wide temperature range of 50–140°C are presented. In addition, the effects of different initiator types and concentrations on the polymerization kinetics and on the molecular weight development are described.

EXPERIMENTAL

The monomer DADC from Akzo Nobel (Arnhem, Germany) and commercial peroxide initiators bis(4-*tert*-butylcyclohexyl) peroxydicarbonate (P16S), dicyclohexyl peroxydicarbonate (CHPC) from Peroxide Chemie GmbH (Munchen, Germany), BPO from Aldrich (St. Louis, MO), and dicumyl peroxide (DCPO) from Hercules (Wilmington, DE) were used.

Samples of approximately 10 mg of the monomer were prepared in tubes at 20°C. An initial amount of the initiator was added to DADC separately, and they were mixed in a nitrogen atmosphere and put in a water bath for polymerization between 50 and 90°C and in an oil bath for polymerization between 100 and 140°C. The initiator concentration varied between 0.1 and 8 wt %. At different reaction times, the samples were quenched on ice and prepared for an analysis.

The C═C bond conversion was measured with FT-Raman and FTIR spectra, which were obtained with a PerkinElmer Spectrum 2000 spectrometer. The spectra were recorded at room temperature in a nitrogen atmosphere after 32 scans at a 2-cm^{-1} resolution. The reference spectra were taken with blank cells under the same conditions. The average C═C bond conversions were calculated from these sets of data, which were obtained in exactly the same way as it was done in the study of O'Donnel and O'Sullivan.[3]

The densities of the DADC monomer were measured at various temperatures with an Erikson pycnometer according to the DIN 53217 standard. The densities were measured up to three times per experiment, and the average values were used.

The molecular weights were measured with a PerkinElmer GPC PL gel mixed E column, with a pore size of 260 nm. Tetrahydrofuran was used as an eluent for different degrees of polymerization. Polystyrene standards were used for the calibration of the molecular weight.

MODEL DEVELOPMENT

The free-radical polymerization of DADC consists of three phases: initiation, propagation, and termination. The main side reactions are degradative chain transfer, after which the reinitiation and stabilization of active radicals occur.[1–6] A detailed reaction pathway composed on the basis of the literature[1–6] is shown in Figure 1. From the reaction pathway, the kinetic scheme for bulk DADC polymerization was proposed, which is shown in Table I, together with corresponding rate expressions for all reaction conditions.

The long-chain hypothesis was applied so that the monomers consumed during the initiation and chain-transfer reactions were ignored. The long-chain radical concentrations were defined by population balance equations, which are summarized in Table II for various polymerization conditions.

The method of moments was used to simplify the infinite number of balance equations.[8,9] The kth moment of living polymer chains (λ_k) and the kth moment of dead polymer chains (μ_k) are defined by

$$\lambda_k = \sum_{i=1}^{\infty} i^k R^{\bullet}_i \qquad (1)$$

TABLE I
Kinetic Scheme of the bulk DADC Polymerization

Initiator decomposition	$I_2 \rightarrow 2I^{\bullet}$	$-r_D = k_D[I_2]$
Initiation of the monomer	$I^{\bullet} + M \rightarrow R^{\bullet}$	$-r_i = 2fk_D[I_2]$
Propagation	$R_n^{\bullet} + M \rightarrow R_{n+1}^{\bullet}$	$-r_p = k_p[R_n^{\bullet}]\,[M]$
Degradative chain transfer	$R_n^{\bullet} + M \rightarrow D_n + A^{\bullet}$	$-r_{Deg} = k_{Deg}[R_n^{\bullet}]\,[M]$
Reinitiation of the monomer	$A^{\bullet} + M \rightarrow R_1^{\bullet}$	$-r_A = k_{ri}[A^{\bullet}]\,[M]$
Active radical stabilization (termination)	$A^{\bullet} + A^{\bullet} \rightarrow D_1$	$-r_{tCh.Tr.} = k_{tCh.Tr.}[A^{\bullet}]^2$
Termination	$R_n^{\bullet} + R_m^{\bullet} \rightarrow D_{n+m}$	$-r_t = k_t[R_n^{\bullet}]\,[R_m^{\bullet}]$

r_D = rate of initiator decomposition; r_{Deg} = rate of degradative chain transfer; r_A = rate of reinitiation; $r_{t\text{Ch.Tr.F}}$ = rate of chain transfer; r_i = rate of initiation; $A^{\bullet}$ = active radical appearing at degradative chain transfer.[1–3,5]

$$\mu_k = \sum_{i=1}^{\infty} i^k D_i \tag{2}$$

where R_i is the i-th macroradical, D_i is the i-th polymer, and i is the counter.

Before the model equations were derived, several common and valid assumptions were made to simplify the kinetic model to some extent: (1) no impurities were present in the reaction mixture, (2) polymerization was homogeneous, (3) the initiator decomposition occurred only with thermal methods, and (4) the cyclization was of minor importance in the polymerization of DADC as reported by Schnarr and Russell.[1] These observations were in addition confirmed by Perera,[7] who investigated the CR-39 polymerization by NMR and reported that only 10% of CR-39 that formed was cyclized. Therefore, the cyclization was not included in the reaction scheme.

The final set of differential equations, which represents the kinetic model equations, is shown in Table III.

In this kinetic model, the cumulative number-average (M_n) and weight-average (M_w) molecular weights were calculated as follows:[8,9]

$$M_n = M_m \frac{[\lambda_2] + [\mu_2]}{[\lambda_0] + [\mu_0]} \tag{3}$$

TABLE II
Population Balance Equations

$$\frac{d[I_2]}{dt} = -k_D[I_2]$$

$$\frac{d[M]}{dt} = -k_p[M]\sum_1^{\infty}[R_i^{\bullet}]$$

$$\frac{d[R_1^{\bullet}]}{dt} = 2fk_D[I_2] - k_p[M]\,[R_1^{\bullet}] - k_t[R_1^{\bullet}]\sum_1^{\infty}[R_i^{\bullet}]$$

$$\frac{d[R_n^{\bullet}]}{dt} = k_p[M]([R_{n-1}^{\bullet}] - [R_n^{\bullet}]) - k_t[R_n^{\bullet}]\sum_1^{\infty}[R_i^{\bullet}] \qquad n>2$$

$$\frac{d[D_n]}{dt} = k_{Deg}[M]\sum_1^{\infty}[R_i^{\bullet}] + k_t\sum_1^{\infty}[R_i^{\bullet}]\sum_1^{\infty}[R_i^{\bullet}]$$

$$M_w = M_m \frac{[\lambda_2] + [\mu_2]}{[\lambda_1] + [\mu_1]} \tag{4}$$

where M_m is the molecular weight of the monomer (274.3). Thus, the propagation and termination rates are subject to diffusion control because of the limited mobility of long-chain radicals caused by the increasing viscosity and chain entanglements.[10]

The apparent propagation (k_p) and termination (k_t) kinetic rate constants are the sum of the inversed values of the chemically controlled constants k_{pc} and k_{tc} and the diffusion-controlled constants k_{pd} and k_{td}, which yield[10]

$$\frac{1}{k_p} = \frac{1}{k_{pc}} + \frac{1}{k_{pd}} \tag{5}$$

$$k_{pd} = 4\pi\bar{r}_p N_A D_m \tag{5a}$$

TABLE III
Kinetic Model Equations

$$\frac{d[I_2]}{dt} = -k_D[I_2]$$

$$\frac{d[M]}{dt} = -k_p[M][\lambda_0]$$

$$\frac{d[\lambda_0]}{dt} = 2fk_D[I_2] - k_t[\lambda_0]^2$$

$$\frac{d[\lambda_1]}{dt} = 2fk_D[I_2] + k_p[M]\,[\lambda_0] - k_{Deg}[M][\lambda_1] + k_r[M][A] - k_t[\lambda_0][\lambda_1]$$

$$\frac{d[\lambda_2]}{dt} = 2fk_D[I_2] + k_p[M]([\lambda_0] + 2[\lambda_1]) - k_{Deg}[M][\lambda_2] + k_r[M][A] - k_t[\lambda_0][\lambda_2]$$

$$\frac{d[A]}{dt} = k_{Deg}[M][\lambda_0] - k_r[M][A] - k_{tCh.Tr.}[A]^2$$

$$\frac{d[\mu_0]}{dt} = k_{Deg}[M][\lambda_0] + k_{tCh.Tr.}[A]^2 + k_t[\lambda_0]^2$$

$$\frac{d[\mu_1]}{dt} = k_{Deg}[M][\lambda_1] + k_{tCh.Tr.}[A]^2 + k_t[\lambda_0][\lambda_1]$$

$$\frac{d[\mu_2]}{dt} = k_{Deg}[M][\lambda_2] + k_{tCh.Tr.}[A]^2 + k_t[\lambda_0][\lambda_2]$$

$$\frac{1}{k_t} = \frac{1}{k_{tc}} + \frac{1}{k_{td}} \tag{6}$$

$$k_{td} = 4\pi\bar{r}_1 N_A D_P \tag{6a}$$

where N_A is Avogadro's number (6.023×10^{23}), r_p is the rate of propagation, r_t is the rate of termination, D_m is the monomer–polymer diffusion coefficient, and D_P is the polymer–polymer diffusion coefficient. Because no critical gel point can be found in the conversion–time curves, the free-volume theory developed by Vrentas et al.[11,12] and Duda et al.[13] was used for the diffusion limitation dependence on the conversion. D_m is expressed as follows:[10–14]

$$D_m = D_{m0} \exp\left[-\gamma \frac{(\omega_m V_m^* + \omega_p V_P^* \zeta)}{V_{FH_m}} \right] \tag{7}$$

where D_{m0} is the initial monomer–polymer diffusion coefficient, γ is the overlap factor (including the shared free volume), ω_m is the weight fraction of the monomer, ω_p is the weight fraction of the polymer, V_m^* is the specific critical hole volume of the monomer, V_p^* is the specific critical hole volume of the polymer, and ξ is the critical molar volume ratio of the jumping unit to the critical molar volume of the polymer. D_P is expressed as[10–14]

$$D_P = D_{P0} \exp\left[-\gamma \frac{(\omega_m V_m^* + \omega_P V_P^* \zeta)}{\zeta V_{FH_P}} \right] \tag{8}$$

where D_{P0} is the initial polymer–polymer diffusion coefficient. By inserting eqs. (7) and (8) into eqs. (5a) and (6a) and by defining the diffusion-controlled constants (k_{pd} and k_{td}) as proposed in recent work by Litvinenko and Kaminsky,[10] we obtained the following equations used for kinetic modeling:

$$k_{pd} = k_{pd0} \exp\left[-\gamma \frac{(\omega_m V_m^* + \omega_p V_P^* \zeta)}{V_{FH_m}} \right] \quad \text{where} \quad k_{pd0} = 4\pi\bar{r}_p N_A D_{m0} \tag{9}$$

$$k_{td} = k_{td0} \exp\left[-\gamma \frac{(\omega_m V_m^* + \omega_P V_P^* \zeta)}{\zeta V_{FH_P}} \right] \quad \text{where} \quad k_{td0} = 4\pi\bar{r}_t N_A D_{P0} \tag{10}$$

where k_{pd0} is the initial diffusion-controlled kinetic rate constant of propagation; k_{td0} is the initial diffusion-controlled kinetic rate constant of termination; and V_{FH_m} and V_{FH_p} are the free volumes for the monomer and polymer, respectively. V_{FH_m} and V_{FH_p} were computed as follows:[10,11–16]

$$V_{FH_m} = \omega_m V_m^* [v_{fm} + \alpha_m (T - T_{gm})] + \omega_P V^*{}_p [v_{fP} + \alpha_P (T - T_{gP})] \tag{11}$$

$$V_{FH_p} = \omega_m V_m^* [v_{fm} + \alpha_m (T - T_{gm})] + \omega_P \delta V^*{}_p [v_{fp} + \alpha_P (T - T_{gP})] \tag{12}$$

where v_{fm} is the free-volume fraction of the monomer, v_{fP} is the free volume of the polymer, α_m is the monomer thermal expansion factor, α_P is the polymer thermal expansion factor, T is the temperature, T_{gm} is the glass-transition temperature of the monomer, and T_{gP} is the glass-transition temperature of the polymer. In addition, the crosslinking factor (δ), defined by Vrentas and Vrentas[15] and obtained from reported density data at various added crosslink concentrations obtained from the study by Stejny,[17] was introduced for recording the dependence of the diffusion coefficient on the crosslinking.[15] A similar δ introduction to V_{FH_p} calculation was proposed for the modeling of diffusion-controlled bulk crosslinking diethylene glycol diacrylate photopolymerizations by Kurdikar and Peppas.[16]

Before the proposed kinetic model could be used to simulate the polymerization process, several physical properties of the initiator, monomer, and polymer needed to be obtained from special experiments.

First, the initiator decomposition rate constants (k_D) for all four initiators were calculated under the assumption of first-order initiator decomposition.[2,4,8] All the necessary kinetic parameters for calculating k_D, which were used for kinetic modeling, were obtained from product information[18] and are reported in Table IV.

Second, the initiator efficiency (f) values for all four initiators were obtained from the theory of dead-end polymerization[19,20] for this initiator–monomer system. The f values were calculated from gel permeation chromatography (GPC) measurements of the M_n values of polymer samples and from conversions measured by FTIR under those conditions; the polymerization was initiated by low initiator concentrations (0.1–1 wt %).[19] The f values were calculated by the least-square fitting of the measured M_n data and the monomer and initiator concentrations as follows:

$$M_n = M_m \frac{[\mathrm{M}_0] - [\mathrm{M}]}{f\{[\mathrm{I}_0] - [\mathrm{I}]\}} \tag{13}$$

where $[\mathrm{M}_0]$ and $[\mathrm{I}_0]$ and $[\mathrm{M}]$ and $[\mathrm{I}]$ denote the monomer and the initiator concentrations at $t = 0$ and t, respectively. Thus, the obtained f values were used for kinetic model simulation. Because of the lack of physicochemical data and because of the complexity of the kinetic modeling, constant f values were assumed throughout the entire polymerization. Similar predic-

TABLE IV
Initiator Decomposition Rate Constants and Measured and Calculated Physical Properties

Initiator decomposition rate constant		
$k_D[s^{-1}] = 4.88 \times 10^{14} \exp\left(-\frac{120.8 \text{ kJ mol}}{RT \text{ [K]}}\right)$	CHPC	Product information[18]
$k_D[s^{-1}] = 4.33 \times 10^{17} \exp\left(-\frac{141.5 \text{ kJ mol}}{RT \text{ [K]}}\right)$	P16S	Product information[18]
$k_D[s^{-1}] = 2.85 \times 10^{12} \exp\left(-\frac{113.2 \text{ kJ mol}}{RT \text{ [K]}}\right)$	BPO	Product information[18]
$k_D[s^{-1}] = 8.38 \times 10^{11} \exp\left(-\frac{120.1 \text{ kJ mol}}{RT \text{ [K]}}\right)$	DCPO	Product information[18]
Measured and calculated physical properties		
ρ_m [g cm^{-3}] = 1.15 − 4.81 × 10^{-4} × T[K]	This work, measured	
ρ_p [g cm^{-3}] = 1.31 − 1.28 × 10^{-4} × T[K]	Product information[24]	
V_m^* = 0.69 cm^3/g	Calculated from Zielinski and Duda[31]	
V_p^* = 0.37 cm^3/g	Calculated from Zielinski and Duda[31]	
M_p = 411.4 g/mol	Calculated from Zielinski and Duda[31]	
α_m = 4.81 × 10^{-4} K^{-1}	This work, calculated from density measurements	
α_p = 1.28 × 10^{-4} K^{-1}	Product information[24]	
T_{gm} = −96°C	Calculated from Fedors[23]	
T_{gP} = 112°C	Stejny[17]	
$v_{fm} = v_{fP}$ = 0.025	Bueche[25]	
ζ = 0.80	Calculated from Zielinski and Duda[31]	
γ = 1	Calculated from Zielinski and Duda[31]	
δ = 0.91	This work, calculated as proposed by Vrentas and Vrentas,[15] measurements obtained from Stejny[17]	

α_m = monomer density; α_p = polymer density; M_p = calculated molecular weight of the jumping unit.

tions were made for kinetic modeling of other polymerization systems.[21,22] The data obtained for f at various DADC bulk polymerization conditions are summarized in Table V.

Third, the kinetic rate constant of degradative chain transfer (k_{Deg}) at various temperatures was obtained with respect to k_p in exactly the same way as proposed in the study by Schnarr and Russell.[1]

The intercept of 1/DP [where DP is the degree of polymerization (M_w/M_n)] versus $r_p/[\text{M}]^2$ gives the k_{Deg}/k_p ratio:

$$\frac{1}{\text{DP}} = \left[\frac{k_{tc} r_p}{k_{pc}^2 [\text{M}]^2}\right] + \frac{k_{\text{Deg}}}{k_p} \tag{14}$$

Thus, the obtained kinetic rate constant ratios were determined by least-square linear fitting of 1/DP to $r_p/[\text{M}]^2$. The obtained slopes give k_{tc}/k_{pc}^2 ratios, and the intercept gives k_{Deg}/k_p under various reaction conditions. All the obtained data were used for kinetic modeling and are reported in Table V for DADC bulk polymerization.

Fourth, for the dependence of the active radical stabilization termination rate constant ($k_{t\text{Ch.Tr.}}$) on the temperature, Arrhenius dependence was assumed. All the necessary kinetic parameters were calculated from the data published on the $k_{t\text{Ch.Tr.}}$ values at different

TABLE V
Initiator Efficiencies, k_{pc}^2/k_{tc} Ratios, and k_{Deg}/k_p for Various Initiator Types, Loadings, and Polymerization Temperatures obtained from Molecular Weight and Conversion Measurements

Initiator type	T (°C)	[I] (mol/L)	f	$(k_{pc}^2/k_{tc}) \times 10^3$ (Ls^{-1} mol^{-1})	$(k_{\text{Deg}}/k_p) \times 10^2$
CHPC	50	0.204	0.71	0.13	0.79
	60	0.120	0.61	0.33	0.98
	60	0.204	0.61	0.33	1.01
	60	0.338	0.61	0.33	1.02
	70	0.204	0.50	0.48	1.12
P16S	50	0.147	0.70	0.13	0.80
	60	0.086	0.64	0.25	0.95
	60	0.147	0.64	0.25	1.04
	60	0.243	0.64	0.25	1.06
	70	0.147	0.52	0.46	1.14
BPO	70	0.242	0.83	0.39	1.22
	80	0.242	0.52	0.79	1.35
	90	0.142	0.46	1.13	1.44
	90	0.242	0.46	1.13	1.52
	90	0.399	0.46	1.13	1.54
	100	0.242	0.43	1.54	1.72
	110	0.242	0.30	2.01	1.92
DCPO	110	0.216	0.60	2.01	1.95
	120	0.127	0.50	2.74	2.15
	120	0.216	0.50	3.15	2.18
	120	0.358	0.50	3.15	2.20
	130	0.216	0.36	3.15	2.42
	140	0.216	0.34	3.64	2.58

reaction temperatures, as reported in the study by Hill et al.,[2] and the following result was obtained:

$$k_{t\text{Ch.Tr.}}\ [\text{Ls}^{-1}\ \text{mol}^{-1}] = 5.54 \times 10^{13} \exp\left(-\frac{34.40\ \text{kJ/mol}}{RT}\right) \quad (15)$$

The $k_{t\text{Ch.Tr.}}$ values were used for kinetic modeling.

Fifth, the values of the reinitiation rate constant (k_{ri}) at different polymerization temperatures were calculated from the ratios of the reinitiation kinetic rate constant to the square root of the active radical termination rate constant at different reaction temperatures for DADC bulk polymerization, as reported by Hill et al.[2] In this study, the Arrhenius temperature dependence of the $(k_{ri}/k_{t\text{Ch.Tr.}})^{0.5}$ ratio was assumed, and the following results were obtained for DADC polymerization:

$$\frac{k_{ri}}{(k_{t\text{Ch.Tr.}})^{0.5}}\ (\text{Ls}^{-1}\ \text{mol}^{-1})^{0.5} = 1.047 \exp\left(-\frac{0.13\ \text{kJ/mol}}{RT}\right) \quad (16)$$

where R is the gas constant (8.314). The kinetic rate constant ratios obtained were used for kinetic modeling.

Sixth, because T_{gm} could not be obtained by DSC measurements, it was calculated with the Fedors correlation.[23] The calculated glass-transition temperature of the DADC monomer was −96°C.

Seventh, T_{gP} was obtained from the study by Stejny,[17] who reported it to be 112°C.

Eighth, thermal expansion factors for the monomer and polymer were used in the proposed kinetic model to calculate the changes in the free-volume fraction during the polymerization. α_m was calculated from the measured density data for the DADC monomer at various temperatures and was found to be 4.81×10^{-4}. α_p was taken from the reported data for the DADC polymer[24] and was 1.28×10^{-4}.

Ninth, the free-volume fraction of the monomer–polymer DADC mixture at the final conversion was 0.025 for both the monomer and polymer, as proposed by Bueche.[25]

Tenth, other transport and physical parameters used in the kinetic model simulations for DADC polymerization were calculated with the predictive method published by Zielinski and Duda[31] and are reported in Table VI.

Computer simulations were done under the assumption of isothermal behavior. The model equations (Table III) were simultaneously solved by the Rosenbrook method.

Although the model requires a large number of parameters, most of the parameters were determined independently, taken from separate experiments of the molecular weight, calculated from glass-transition temperatures, or taken from other references. By fitting the model to measured conversions, we obtained only two temperature-dependent kinetic parameters (k_{pd0} and k_{td0}) with the Levenberg–Marquardt algorithm.

TABLE VI
Simulation Results Obtained from Model Fitting for Bulk DADC Polymerization

Initiator type	T (°C)	[I] (mol/L)	$k_{pd0} \times 10^{-9}$ (L mol^{-1} s^{-1})	$k_{td0} \times 10^{-15}$ (L mol^{-1} s^{-1})
CHPC	50	0.204	0.10	1.69
	60	0.120	0.11	1.88
	60	0.204	0.11	1.91
	60	0.338	0.12	1.92
	70	0.204	0.17	1.93
P16S	50	0.147	0.11	1.69
	60	0.086	0.11	1.87
	60	0.147	0.11	1.91
	60	0.243	0.12	1.93
	70	0.147	0.17	1.93
BPO	70	0.242	0.17	1.93
	80	0.242	0.21	2.77
	90	0.142	0.35	3.98
	90	0.242	0.36	4.00
	90	0.399	0.36	4.03
	100	0.242	1.00	5.03
	110	0.242	3.69	9.43
DCPO	110	0.216	3.44	20.00
	120	0.127	3.55	63.62
	120	0.216	3.56	63.69
	120	0.358	3.58	63.74
	130	0.216	4.57	72.99
	140	0.216	5.12	81.11

RESULTS AND DISCUSSION

In this section, the kinetic parameters are presented and discussed in detail; model predictions are compared with experimentally measured data for the conversions for isothermal batch DADC polymerization at different reaction temperatures, various initiator types, and different loadings.

The f values were calculated from the dead-end polymerization with a simple reaction scheme, which consisted only of the initiation, propagation, and termination reactions. Special experiments were carried out with low initiator loadings (0.1–1 wt %), at which it was assumed that no diffusion limitations appeared.[19] The f values at various temperatures are shown in Table V and were used for kinetic modeling. The f values for all four initiator types varied with the reaction temperature between 0.3 and 0.83; this was similar to the results obtained for other systems.[14,26] In general, the f values decreased with an increase in the reaction temperature. In addition, by comparing the f values for two initiators at the same polymerization temperatures, we observed that f depended on the type of initiator used (CHPC and P16S). Thus, the obtained f values for the CHPC initiator

were similar to the results reported by Van Sickle,[27] who studied the synthesis, thermal decomposition, and f values in various solvents. The f values obtained for the BPO initiator varied between 0.3 and 0.83, and this was in agreement with the results obtained from the study of Ray et al.,[28] who studied MMA (methyl methacrylate) kinetic modeling.

The k_{Deg}/k_p ratios were determined from average molecular weight measurements of the samples up to the gel point (20–25% conversion) until there was sufficient solubility of the polymer. The obtained k_{Deg}/k_p ratios are shown in Table V. The ratios increased with the reaction temperature; this was similar to the results obtained from the study of bulk diallyl terephthalate (DAT) monomers by Matsumoto and coworkers,[5,6] from the kinetic modeling of bulk DAT polymerization,[29] and from the results reported for other systems.[30] From the calculated results for the k_{Deg}/k_p ratios at various temperatures, it may be assumed that at higher reaction temperatures, the degradative chain-transfer reaction was favored with respect to the propagation reaction. The chain-transfer ratios ranged from 7.9×10^{-3} to 2.5×10^{-2}, which was in good agreement with the results obtained by Russell and Schnarr,[1] who reported the chain-transfer ratio to be around 1.4×10^{-2}. The differences between the k_{Deg}/k_p ratios at the same reaction temperature (50–70°C) for CHPC and P16S initiators, 70°C for CHPC, P16S, and BPO and 110°C for BPO and DCPO initiators, were probably the results of the different initiator types used. The chain-transfer ratios obtained in this study were plotted against the temperature under the assumption of Arrhenius temperature dependence for all four initiators, and the following result was obtained:

$$\frac{k_{\mathrm{Deg}}}{k_p} = (1.67 \pm 0.1) \exp\left(- \frac{14.2 \pm 0.2 \text{ kJ/mol}}{RT} \right) \quad (17)$$

For kinetic modeling, the determined chain-transfer ratio was used.

The k_{pc}^2/k_{tc} ratios were obtained from measured M_n's and are shown in Table V for various reaction conditions. k_{pc}^2/k_{tc} ratios increased with the temperature, and this agreed with the results obtained from other kinetic studies by Gu et al.[21] for *N*-vinylformamide bulk and solution polymerization and with the results reported by Mayo et al.[30] From the obtained data for kinetic rate constant ratios for different initiator types at the same polymerization temperature (e.g., CHPC and P16S), similar ratio values could be observed, and this agreed with the reported measurements from other systems.[30] The differences could be attributed to the different initiators used. The obtained k_{pc}^2/k_{tc} kinetic constant ratios were between 1.3×10^{-4} and 3.64×10^{-3} under various reaction conditions. The k_{pc}^2/k_{tc} ratios were similar to the results obtained from the study of bulk DAT polymerization by Hace et al.[29] and the results reported for bulk MMA polymerization.[8,9,14]

In the following step, the initial $\ln(-r_p/[I_2]^2)$ values were plotted against the initiator concentrations ($[I_2]$), and fairly good straight lines were obtained in all runs; this agreed with the results reported by Schnarr and Russell.[1] The temperature dependence of the slopes corresponded to an apparent activation energy of 37.6 kJ mol^{-1}. In addition, the calculated $-r_p$ value for DADC polymerization at 90°C with 5 wt % BPO (initiator) was calculated to be 1.3×10^{-4} mol s^{-1} L^{-1}. It was in good agreement with the $-r_p$ value reported by Hill et al.,[2] who used exactly the same reaction conditions; that value was reported to be 1.5×10^{-4} mol s^{-1} L^{-1}. The differences were attributed to different analytical techniques used for the extent of the DADC polymerization measurements. Hill et al.[2] in their study, used the ESR technique to measure the radical concentrations.

From the glass-transition temperatures (T_{gm} and T_{gP}) and other physical properties of the monomer and polymer, the parameters for free-volume theory were calculated as proposed by Zielinski and Duda.[31] The results are reported in Table IV, along with other calculated kinetic parameters used for kinetic model fitting and reported references for comparison.

The remaining two kinetic parameters (k_{pd0} and k_{td0}) with clear and physical meaning were obtained from kinetic model fitting to the measured conversion–time curves. Their values are reported in Table VI and depend on the reaction temperature only. From the calculated k_{pd0} and k_{td0} values at the same reaction temperatures for two initiator types (CHPC and P16S), no strict dependence on the type of initiator was observed, and this agreed with the nature of diffusion.[8,10] The k_{pd0} and k_{td0} values were around 10^9 and 10^{15} L mol^{-1} s^{-1}, respectively. The values were higher than the values reported for *N*-vinylformamide bulk polymerization (10^7 L mol^{-1} s^{-1})[21] and slightly lower than the values obtained in the studies of Seth and Gupta[8] and Hoppe and Renken[9] for MMA bulk polymerization (10^{18}–10^{21} L mol^{-1} s^{-1}). The differences were probably due to the different algorithms used for diffusion limitation predictions, different reaction temperatures, and different monomer types. In addition, in DADC polymerization, crosslinking occurs, which is not typical for MMA and *N*-vinylformamide polymerization. The obtained values of both diffusion-controlled kinetic parameters were in good agreement with the results of the study of Hace et al.[30] (10^9 and 10^{16} L s^{-1} mol^{-1}) for DAT bulk polymerization, for which a similar algorithm for the diffusion limitation predictions was used for kinetic modeling. In this study, an Arrhenius dependence of k_{pd0} and k_{td0} on temperature is proposed, and the results are reported as follows:

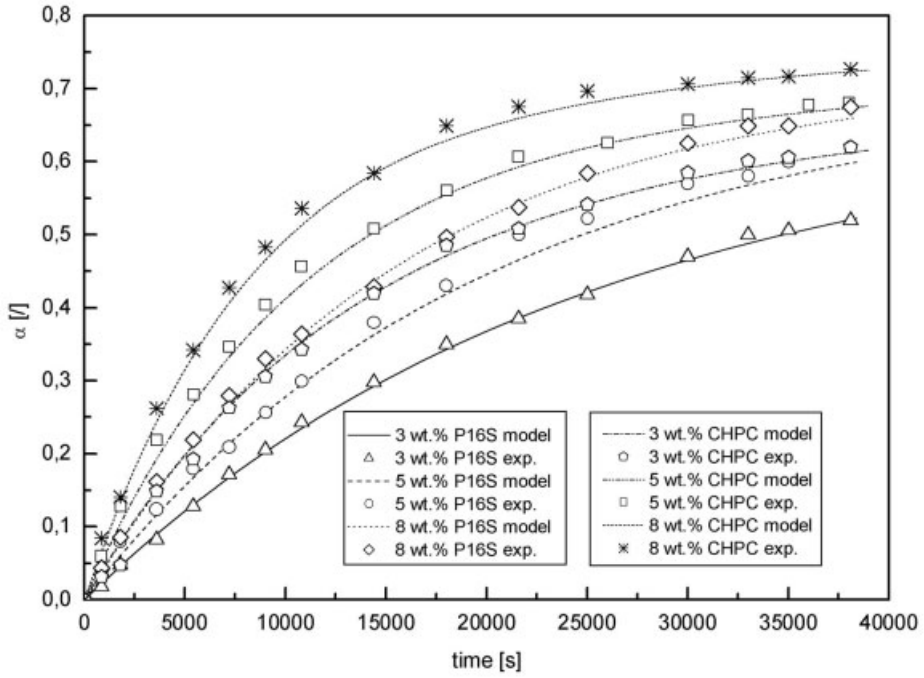

(a)

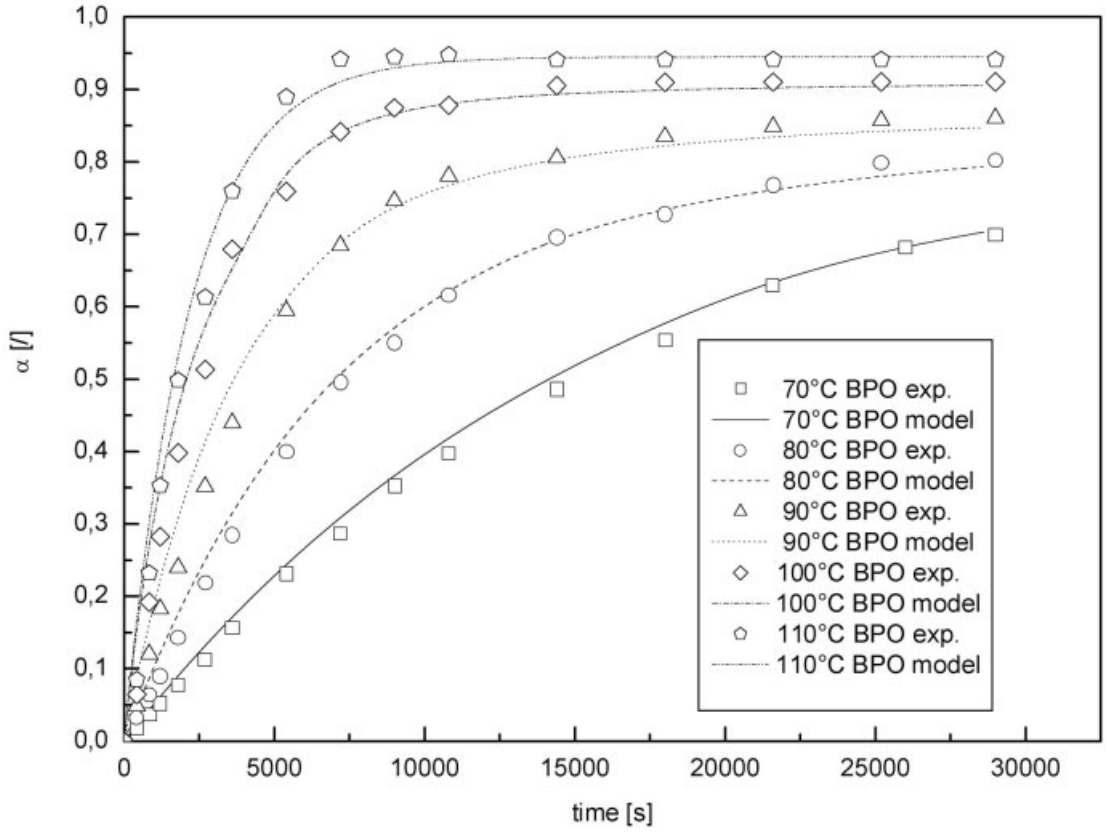

(b)

Figure 2 Comparison of the model simulation and experimental data (a) for 5 wt % CHPC and P16S, (b) for 5 wt % BPO, (c) for 5 wt % DCPO, and (d) for polymerization at 60°C and 3, 5, or 8 wt % CHPC and P16S.

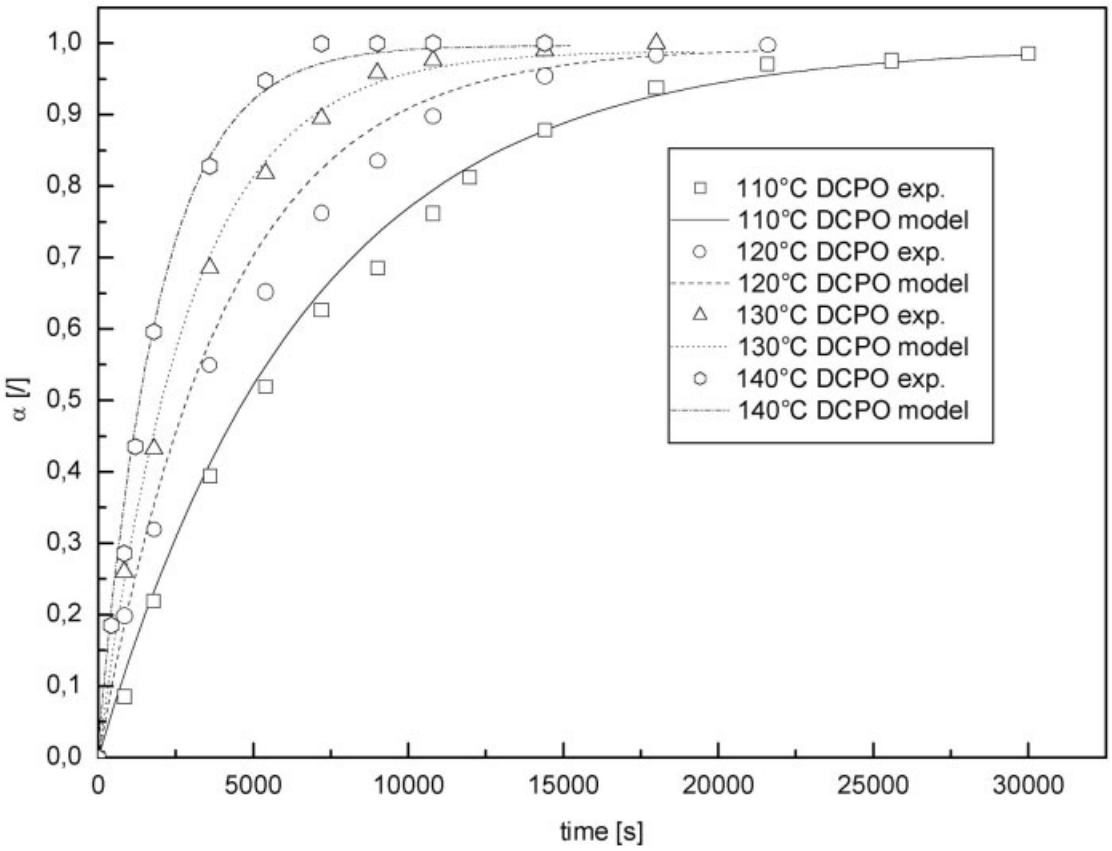

(c)

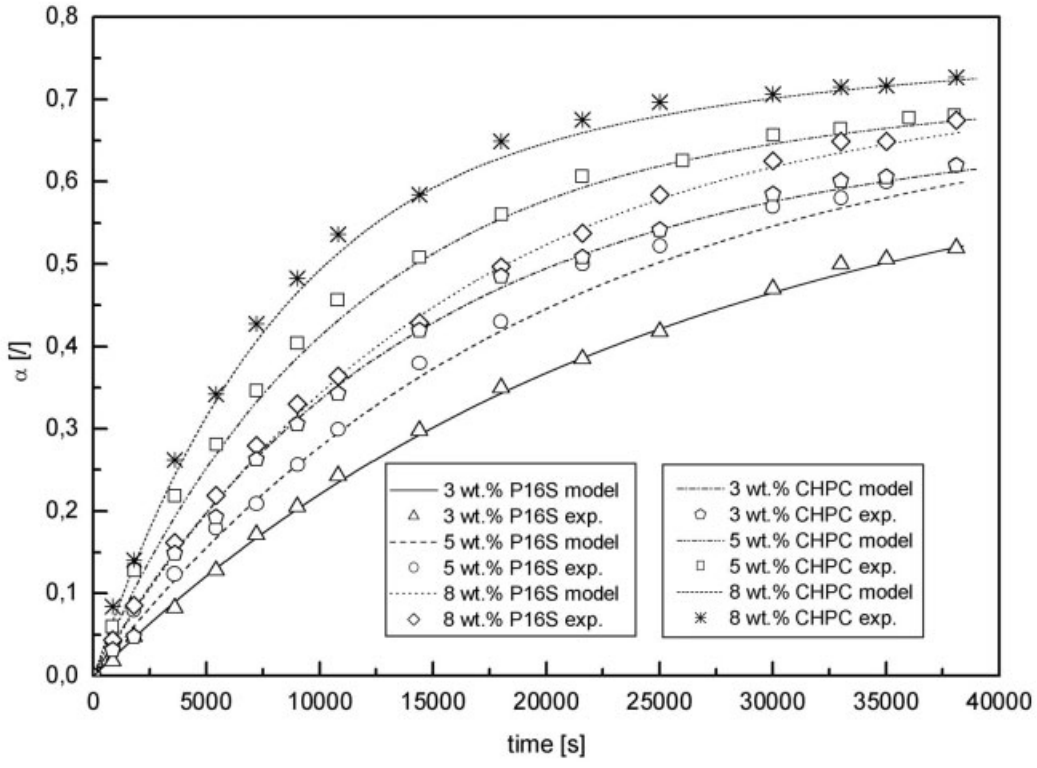

(d)

Figure 2 (*Continued from the previous page*)

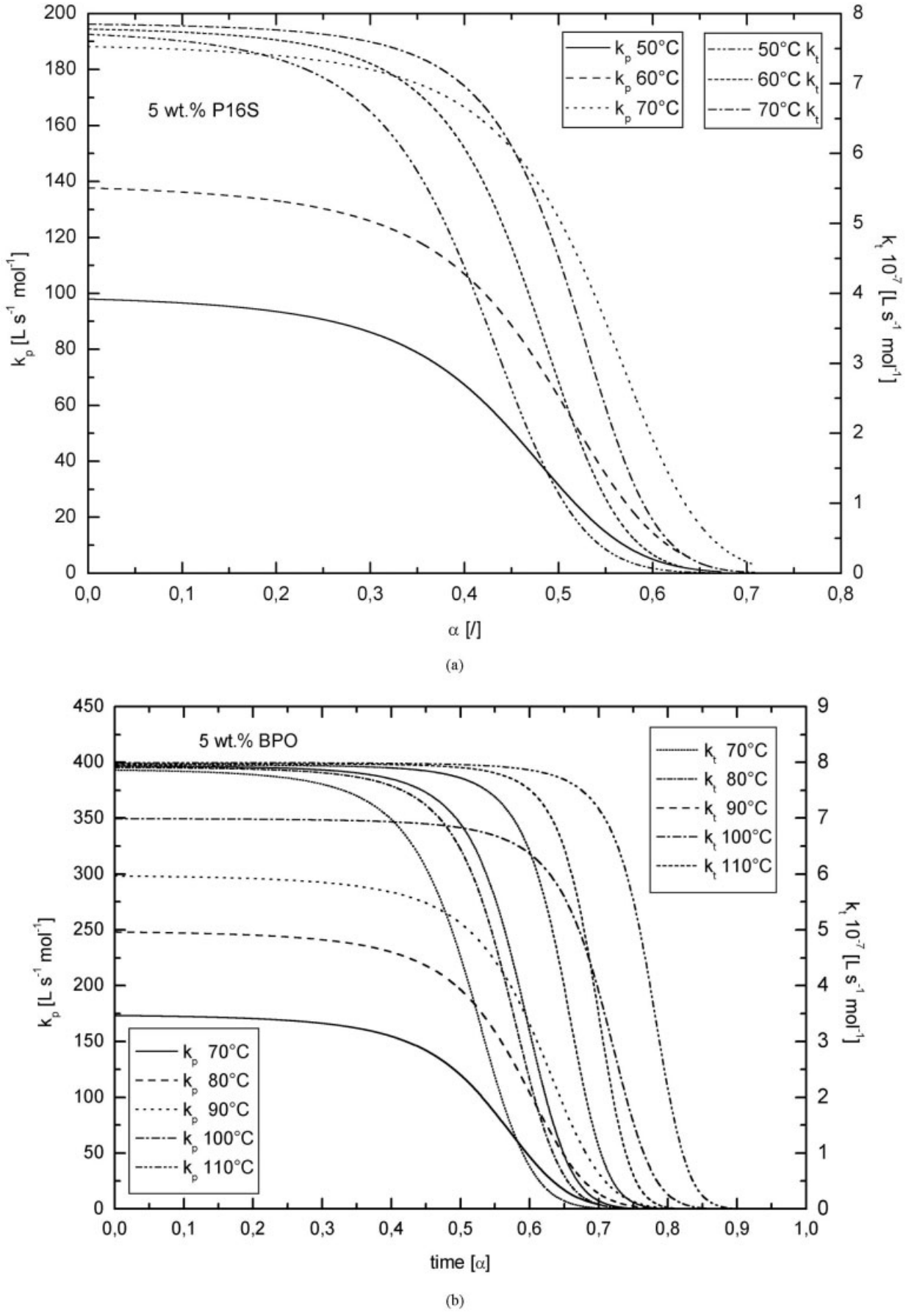

Figure 3 Apparent k_p and k_t rate constants for a 5 wt % initiator loading of (a) P16S and (b) BPO.

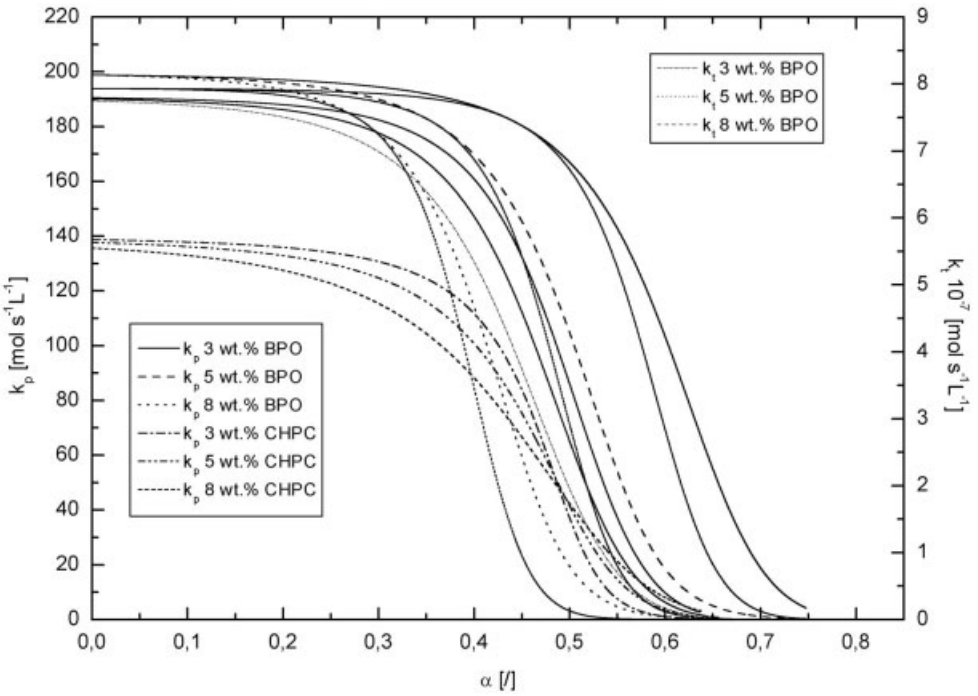

Figure 4 Apparent k_p and k_t rate constants for various initiator loadings of CHPC at 60°C and of BPO at 90°C.

$$k_{pd0}(\mathrm{Ls^{-1}\,mol^{-1}}) = (1.7 \pm 0.1) \times 10^{17} \exp\left(-\frac{58.5 \pm 1.3\ \mathrm{kJ/mol}}{RT}\right) \quad (18)$$

$$k_{td0}(\mathrm{Ls^{-1}\,mol^{-1}}) = (3.8 \pm 0.9) \times 10^{23} \exp\left(-\frac{53.4 \pm 2.6\ \mathrm{kJ/mol}}{RT}\right) \quad (19)$$

By comparing k_{pd0} and k_{td0} values at a constant temperature at different initiator concentrations (Table VI), we can observed that the two kinetic parameters do not show a strict dependence on the initiator concentration. The values remain almost the same for all three different initiator loadings (3, 5, and 8 wt %), and this agrees with results reported for other polymerization systems.[10,21,26,28,32]

A comparison between the conversions predicted by the kinetic model and the experimentally measured ones for various reaction conditions are shown in Figure 2. The proposed kinetic model successfully predicted the measured conversions for all reaction temperatures, types of initiators, and initiator concentrations.

The calculated apparent k_p and k_t values as functions of conversion at different reaction temperatures for 5 wt % P16S and BPO initiators are shown in Figure 3. A similar dependence for both apparent rate constants on the conversion was also observed for CHPC and DCPO initiators (the corresponding diagrams are available upon request). The apparent rate constants decreased from the beginning of the polymerization, and this may have been due to strong diffusion control of the reaction. Similar observations were made for the kinetic modeling of bulk crosslinking diethylene glycol diacrylate photopolymerization reactions by Kurdikar and Peppas[16] and other multifunctional thermally initiated and photoinitiated vinyl monomers.[32] Apparent k_t values decreased earlier than apparent k_p's, and so autoacceleration of the polymerization occurred.[14] Apparent k_p values remained unchanged when the polymerization was controlled by segmental diffusion but began to decrease when translation diffusion became the rate-controlling step. In the later stages of the reaction, the calculated values of k_p and k_t became similar because propagation diffusion was the only mode available for radical movement.[16] The calculated results of k_p and k_t from this model agreed with this theory.

The influence of various initiator concentrations on the apparent kinetic rate constants is shown in Figure 4 for 5 wt % CHPC and BPO initiators. Similar results were obtained for P16S and DCPO initiators. The corresponding diagrams are available upon request. It is apparent that at higher initiator concentrations, the reduction of k_p and k_t with respect to lower initiator concentrations started later. This may be explained by the average chain length reduction with an initiator concentration increase.[10] Therefore, it may be assumed that the initiator concentration affected the reduction of the rate constant in this diffusion-controlled reaction. Similar observations were obtained for bulk MMA polymerization by Achilias and Kiparissides[14] and for other multifunctional diffusion-controlled polymerizations.[16,29,32]

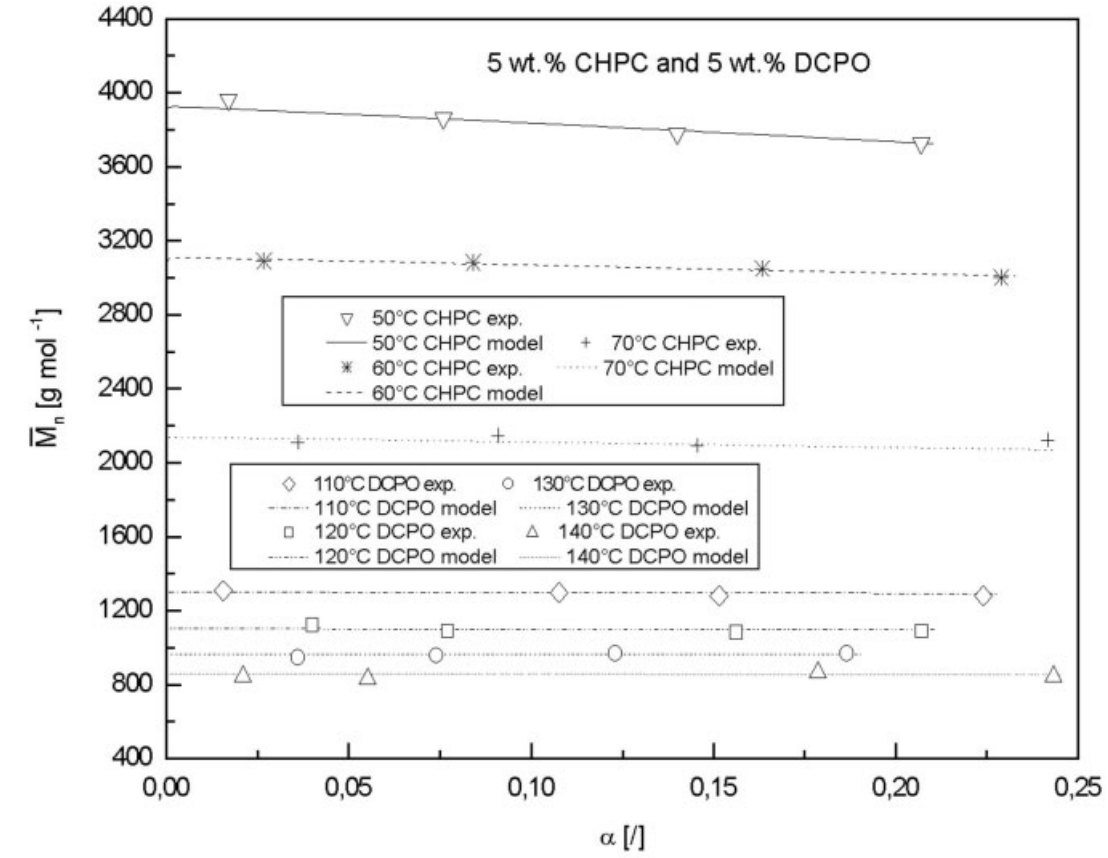

(a)

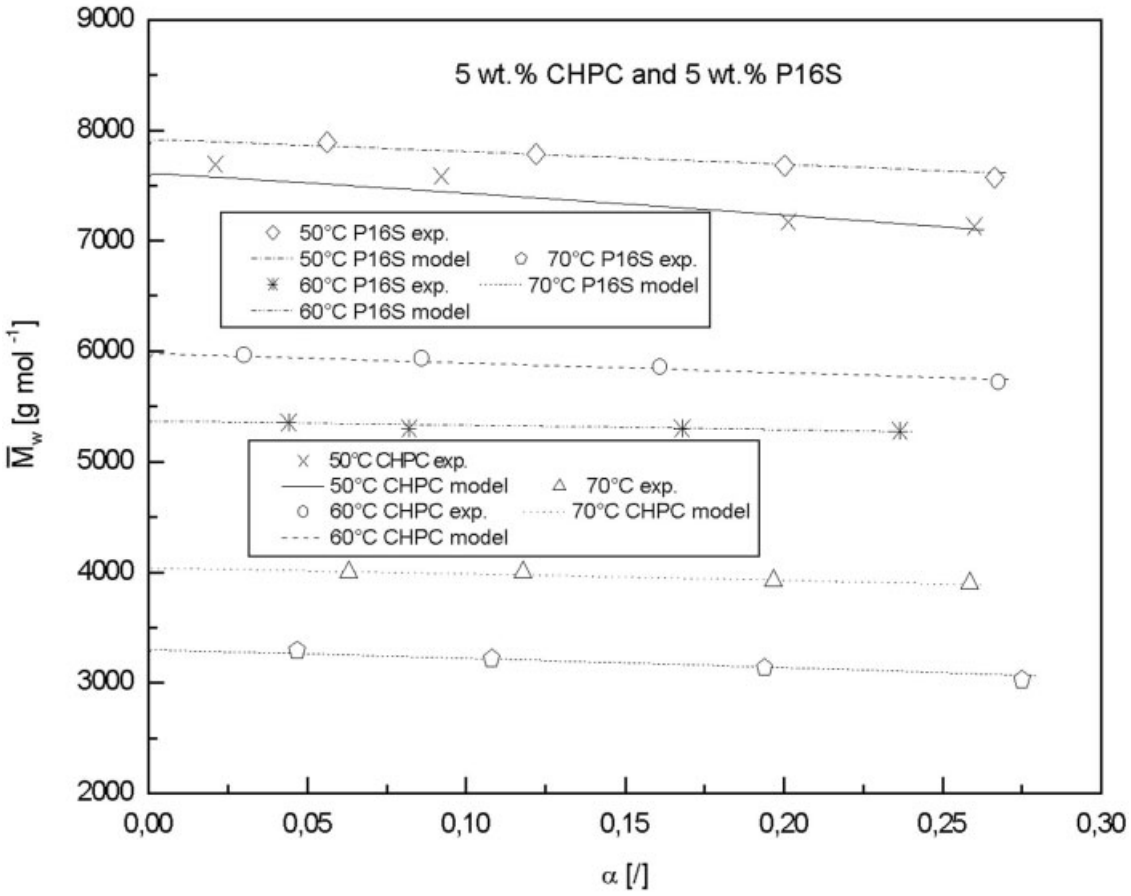

(b)

Figure 5 Comparison of model and experimental (a) M_n values for 5 wt % CHPC and DCPO initiators and (b) M_w values for 5 wt % CHPC and P16S initiators.

From the obtained chemically controlled rate constants (k_{pc} and k_{tc}), the activation energies and pre-exponential factors of intrinsic k_p's and k_t's were determined from an Arrhenius plots of ln k_{pc} and ln k_{tc} versus $1/T$, respectively. The activation energy for the propagation reaction was 21.1 ± 0.9 kJ mol^{-1}, and for termination it was 0.8 ± 0.01 kJ mol^{-1}. Similarly low termination activation energies with respect to propagation were observed in other diffusion-controlled polymerizations.[8–10,14,16,32] Theoretically, the termination activation energy in diffusion-controlled polymerizations may even be zero because of strong diffusion controll.[10] The corresponding pre-exponential factors are 2.93 ± 0.30 × 10^5 and 9.79 ± 0.28 × 10^7 L mol^{-1} s^{-1} for propagation and termination, respectively. The propagation activation energy obtained from our study for bulk DADC polymerization was lower than the values obtained by Schnarr and Russell,[1] who reported the apparent activation energy to be 121.6 kJ mol^{-1}. In the study by O'Donnel and O'Sullivan,[3] the activation energy for the first-order DADC kinetics was reported to be 104 kJ mol^{-1}. The differences may be attributed to a different reaction scheme used for kinetic model development. The propagation activation energy (21.1 kJ mol^{-1}) obtained in this study was similar to the propagation activation energy for bulk DAT polymerization, for which it was reported to be 26 kJ mol^{-1}. The differences were attributed to the different types of monomers.

The M_n's for 5 wt % CHPC and P16S initiators and the M_w's for 5 wt % CHPC and DCPO initiators were calculated from the solutions of kinetic model equations and measured M_n and M_w data up to the gel point and are shown in Figure 5. In general, good agreements between the calculated and experimentally measured M_n and M_w values were obtained. Because of the insufficient solubility of the samples, we were unable to measure the molecular weights after the gel point (20–25% conversion). Nevertheless, the developed kinetic model can successfully predict the polymerization behavior for M_n and M_w well in the pregel stage of polymerization for all four initiators used.

The polydispersities calculated from the M_n and M_w measured data at different reaction temperatures at the gel point varied between 1.72 and 1.95 in all runs in all four initiator types. The obtained polydispersities agreed well with the data reported by Schnarr and Russell[1] (1.7 ± 0.1), which were determined by membrane osmometry and confirmed by GPC measurements.

CONCLUSIONS

The free-radical polymerization of DADC in bulk was examined. With the proposed kinetic model, it was possible to predict measured conversions through the entire DADC polymerization.

On the basis of this study, the following conclusions were made. The activation energies of kinetic rate constants for propagation and termination reactions were determined. Their values were 21 kJ mol^{-1} for propagation and 0.8 kJ mol^{-1} for termination. k_{Deg}/k_p and k_{pc}^2/k_{tc} were obtained with molecular weight measurements from 50 to 140°C in the pregel stage, which was reported to be at approximately 25% conversion. k_{Deg}/k_p values varied between 7.9 × 10^{-3} and 2.5 × 10^{-2}, and this was in good agreement with the results obtained by Schnarr and Russell.[1] k_{pc}^2/k_{tc} varied between 1.3 × 10^{-4} and 3.64 × 10^{-3} L mol^{-1} s^{-1}. In addition, all the obtained kinetic constant ratios increased with the reaction temperature.

The f values for the reported initiator–monomer system were calculated from special experiments with the dead-end theory developed by Tobolsky[19] and were between 0.71 and 0.50 for CHPC, 0.70 and 0.52 for P16S, 0.83 and 0.30 for BPO, and 0.60 and 0.34 for the DCPO initiator at various polymerization temperatures.

References

1. Schnarr, E.; Russell, K. J Polym Sci Polym Chem Ed 1980, 18, 913.
2. Hill, D. J. T.; O'Donnell, H. J.; Perera, M. C. S.; Pomery, P. J. Eur Polym J 1997, 33, 1353.
3. O'Donnell, J. H.; O'Sullivan, P. W. Polym Bull 1981, 5, 103.
4. Hill, D. J. T.; O'Donnell, H. J.; Perera, M. C. S.; Pomery, P. J. Eur Polym J 1997, 33, 649.
5. Matsumoto, A.; Takashima, K.; Oiwa, M. Bull Chem Soc Jpn 1969, 42, 1959.
6. Matsumoto, A. Prog Polym Sci 2001, 26, 189.
7. Perera, M. C. S. Eur Polym J 1999, 35, 997.
8. Seth, V.; Gupta, S. K. J Polym Eng 1995, 15, 284.
9. Hoppe, S.; Renken, A. Polym React Eng 1998, 6, 1.
10. Litvinenko, G. I.; Kaminsky, V. A. Prog React Kinet 1994, 19, 139.
11. Vrentas, J. S.; Duda, J. L.; Ling, H. C. J Polym Sci Polym Phys Ed 1985, 23, 275.
12. Vrentas, J. S.; Duda, J. L.; Ling, H. C. J Polym Sci Polym Phys Ed 1985, 23, 298.
13. Duda, J. L.; Vrentas, J. S.; Ju, S. T.; Lin, H. T. AIChE J 1985, 28, 279.
14. Achilias, D. S.; Kiparissides, C. Macromolecules 1985, 25, 3739.
15. Vrentas, J. S.; Vrentas, C. M. J Appl Polym Sci 1991, 42, 1931.
16. Kurdikar, D. L.; Peppas, N. A. Macromolecules 1994, 27, 4084.
17. Stejny, J. Polym Bull 1996, 36, 617.
18. Noury Initiators (Product Information), Akzo Chemie America: Chicago, IL, 1986.
19. Tobolsky, A. W. J Polym Sci 1958, 80, 5927.
20. Gobran, R. H.; Berenbaum, M. B.; Tobolsky, A. V. J Appl Polym Sci 1960, 46, 434.
21. Gu, L.; Zhu, S.; Hrymak, A. N.; Pelton, R. H. Polymer 2001, 43, 3077.
22. Chen, Z.; Pauer, W.; Pruss, H. U.; Warnecke, H. J. Chem Eng Technol 1999, 22, 609.
23. Fedors, R. F. J Polym Sci Polym Lett Ed 1979, 17, 719.
24. CR-39 (Product Information), PPG Industries, Inc.: Pittsburgh, PA, 2003.
25. Bueche, F. Physical Properties of Polymers; Interscience: New York, 1962.
26. Russell, G. T.; Napper, D. H.; Gilbert, R. G. Macromolecules 1988, 21, 2141.
27. Van Sickle, D. E. J Org Chem 1969, 11, 3446.
28. Ray, A. B.; Saraf, D. N.; Gupta, S. K. Polym Eng Sci 1995, 35, 1290.
29. Hace, I.; Golob, J.; Krajnc, M. Polym Eng Sci 2004, 44, 2005.
30. Mayo, F. R.; Gregg, R. A.; Matheson, M. S. J Am Chem Soc 1951, 73, 1691.
31. Zielinski, J. M.; Duda, J. L. AIChE J 1992, 38, 405.
32. Andrzejewska, E. Prog Polym Sci 2001, 26, 605.